

1 **The potential of low-frequency AVL data for the**
2 **monitoring and control of bus performance**

3 Corresponding author: Yingxiang Yang
4 yxyang@mit.edu

5 David Gerstle
6 dgerstle@mit.edu

7 MIT, Civil and Environmental Engineering Department,
8 77 Massachusetts Avenue, Cambridge, MA, USA

9 Peter Widhalm
10 peter.widhalm@ait.ac.at

11 Dietmar Bauer
12 Dietmar.Bauer@ait.ac.at
13 AIT Austrian Institute of Technology, Department Mobility
14 Dynamic Transportation Systems
15 Giefinggasse 2, A-1210 Wien, Austria

16 Marta Gonzalez
17 martag@gmail.com
18 MIT, Civil and Environmental Engineering Department,
19 77 Massachusetts Avenue, Cambridge, MA, USA

20 4854 words + 10 figures + 0 tables = 7354
21 November 14, 2012

1 **ABSTRACT**

2 In this paper we investigate the potential of "low-frequency" bus localization data for the mon-
3 itoring and control of bus system performance. We show that data with a sampling rate as low
4 as one minute, when processed appropriately, can provide ample information. In particular, we
5 obtain accurate estimates of stop arrival and departure times which in turn allow the analysis of
6 headways and travel times. A three parameter gamma family of distributions is fitted for headways
7 at the stops along a bus line. The evolution of the parameters demonstrates critical points on the
8 line where bus bunching is significantly increased. Moreover, this analysis allows to differenti-
9 ate problems associated with varying passenger demand from uncertainties associated with traffic
10 conditions. Furthermore we show that both expected travel time and travel time variability can be
11 calculated from low-frequency localization data. Finally, we present how our results can be used
12 to calibrate a simulation model which can test bus control strategies. We apply and validate the
13 methods to data obtained from bus route number 1 in Boston.

1 INTRODUCTION

2 Modern advanced traveler information systems (ATIS) are capable of providing information on
3 expected travel times for all modes and origin-destination pairs in real time by incorporating many
4 different data sources including past measurements of vehicle trajectories, passenger demands and
5 current traffic conditions. However, collecting these data is still costly and many data sources are
6 not universally available. In particular automatic fare collection (AFC) or boarding and alighting
7 counts are currently not available in many systems, whereas automatic vehicle location (AVL) in-
8 formation is widespread.

9 However, many AVL systems provide location-at-time data with a low sampling frequency (on
10 the order of a minute). In this situation travel time prediction and bus arrival time prediction can
11 only be based on such AVL data sets. Nextbus is a major provider of AVL data services to transit
12 agencies across North America and offers those agencies web services so that agencies can release
13 their data to the public. The agencies control the amount, quality, and frequency of the updates,
14 and many agencies chose to provide low-frequency data due to budget constraints. These AVL da-
15 ta are also used by transit agencies to evaluate their transit system performance, diagnose service
16 bottlenecks, and improve the system level of service [1, 2].

17 The main limitation of AVL data are measurement errors due to the GPS devices and
18 recording or transmission errors. The low sampling frequency implies that stop dwell times and
19 on-route travel times are not trivial to separate. Linear interpolation methods that are often used
20 (see e.g. Byon et al. [3] and Cortés et al. [4]) distort travel speed and headway measurements
21 significantly. Therefore better alternatives are desirable. Hence in this paper we introduce a new
22 methodology for re-sampling of low frequency location-at-time AVL records.

23 Using the re-sampled data, we perform analysis on transit service quality. Among all the
24 service quality measurements, headway distribution [5, 6], adherence to schedule and in-vehicle
25 travel time are the most studied [7]. For high frequency urban transit service, headway distribution
26 is the measurement directly related to operations [5, 8]. It determines passengers' experienced
27 waiting time and could be effectively improved by operational strategies such as holding and stop
28 skipping [9, 10]. Here we choose to study the variation in the distribution of headway across the
29 entire route as a proxy of the deterioration in service quality.

30 In particular in this paper our goals are threefold:

- 31 • to provide a more accurate data preprocessing methodology which enhances low fre-
32 quency AVL data (see section 2)
- 33 • to show that the such obtained data can be used to evaluate bus service quality (including
34 travel time uncertainty) and diagnose service bottlenecks (see section 3)
- 35 • to use the acquired statistics to calibrate a bus movement model, which subsequently can
36 be used to evaluate different control strategies for mitigating bus bunching effects (see
37 section 4).

38 To achieve these goals, first map-matching is performed on low-frequency location-at-time AVL
39 data to assign transit vehicles to their route shapes. Second, re-sampling is performed incorporating
40 both buses' actions of traveling on route segment and staying at stops. Stop arrival and departure
41 times are inferred. Based on the interpolated data, we then derive statistics of in-vehicle travel
42 time and show how bus headway deviation propagates along the route. We identify bottlenecks

1 and investigate the underlying causes. We provide methods to estimate route travel time and travel
2 time variability. Finally we show how the results could be used to calibrate bus movement models.

3 **2 DATA PREPOSSESSING**

4 In this paper location-at-time AVL data provided by the Nextbus service is used. NextBus, Inc.,
5 provides data for a large number of US and Canadian transit companies (including LA Metro,
6 MBTA, NYC MTA, San Francisco Muni, and the Toronto Transit Commission). The Nextbus
7 server is polled every 60 seconds and returns the bus locations. Additionally, schedule and route
8 information are given in the form of general transit feed specification (GTFS) format introduced
9 by Google. Locations of bus stops from the GTFS are used in order to derive arrival and departure
10 times from the AVL records.

11 To illustrate our methodology, we analyze the AVL records between May 1st 2011 and
12 June 15th 2011 from the route 1 of the MBTA (Massachusetts Bay Transit Authority), totalling
13 4624 trips during weekdays and 796 trips on weekends. MBTA route 1 runs from Dudley station
14 in Boston to Harvard university in Cambridge. The outbound and inbound stops near Harvard
15 university are not symmetric because of the one way streets. The data we used contains outbound
16 runs' records which have 33 stops starting at Dudley station and ending at Quincy St at Harvard
17 St. The average distance between stops is about 250m. A map of MBTA route 1 is shown in Fig.
18 1 where also significant stops are indicated: between stops 8 and 9 the route turns into a main
19 arterial. Between stop 18 and 19 there are 3 intersections and the bus transfers with a metro line
20 here. At stops 12 and 25 large traffic volumes during peak hours are observed.

21 The scheduled headway during morning peak hours equals 8-9 minutes, during the after-
22 noon peak 7-8 minutes while at off-peak times a 12 to 13 minute interval is scheduled.

23 **2.1 Map-matching**

24 The first step in the data preprocessing is map-matching, see Quddus et al. [11] for an up-to-date
25 review.

26 In the data set at hand map-matching has to deal with the following most frequent problems:

- 27 1. Wrong temporal order: time stamp and location pairs appear to be in the wrong order.
28 This makes buses appear to be going backwards along the shapes.
- 29 2. No matching from the shape: the locations provided in AVL records are far from the
30 route shape. Such points occur in particular at the start or the end of trips.
- 31 3. Wrong interval: some trips only have a few data points recorded at irregular intervals.
32 This may indicate the buses are out of service or the GPS devices are broken.

33 We found that on average 97.6% of the observations could be map-matched directly. For the
34 rest 2.4% erroneous observations, 0.6% could be fixed using obvious heuristics, which are mainly
35 wrong temporal order observations. 1.8% of the observations are finally discarded, two thirds of
36 which correspond to a no matching from the shape.

37

38 **2.2 Re-sampling procedure**

39 The output of the map-matching procedure are sequences of $(t_{i,j}, x_{i,j})$ pairs ($t_{i,j}$: time stamp for j -
40 th observation of trip i , $x_{i,j}$: distance along shape) sequences for all trips on a given shape for given

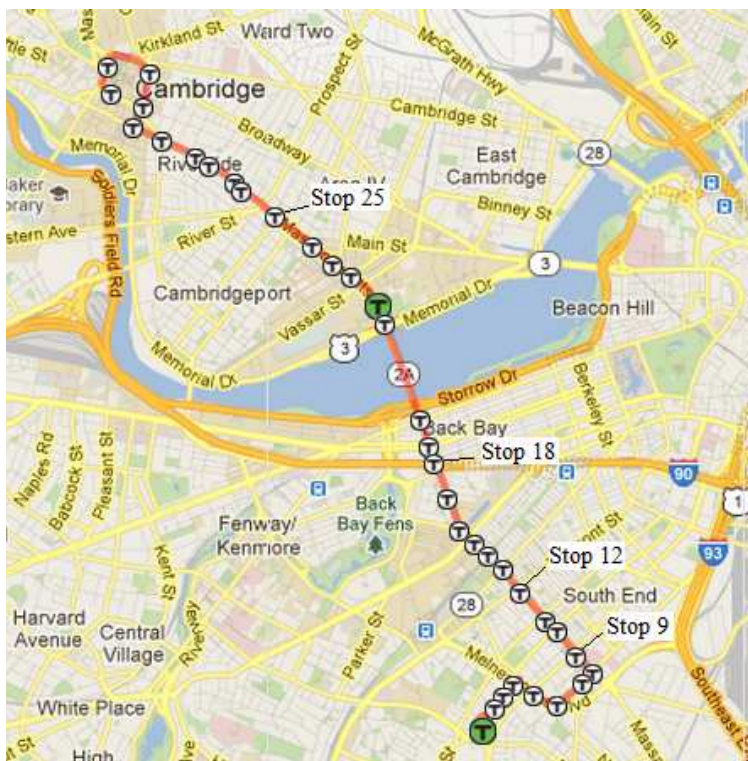


FIGURE 1 MBTA route 1: Significant stops discussed in the text are marked. Map obtained from Google maps.

1 route. Since the GPS tracks of the AVL data is only available approximately every 60 seconds a
 2 re-sampling scheme has been used in order to obtain information on arrival and departure times
 3 at stop locations. For the re-sampling two different approaches could be followed: Viewing time
 4 as a function of the distance along the shape, re-sampling may use interpolation (e.g. linear) or
 5 smoothing methods such as spline smoothing. This has the disadvantage that the result reflects
 6 the properties of the interpolation scheme which might not be desirable. E.g. in the case of three
 7 consecutive observations of a bus, the middle one occurring while the bus was in a stop s (defined
 8 as a small interval $[X(s) - G, X(s) + G]$ around the stop location $X(s)$ according to the shape of
 9 length, $2G = 30\text{m}$) while the remaining two are on the road linear interpolation implies that the bus
 10 is at the stop only for a short duration. For spline smoothing the stopping time will depend heavily
 11 on the smoothing parameter. This behavior clearly is undesirable.

12 As an alternative explicit modeling of bus travel explains time $t(x)$ as a function of distance
 13 along shape x . The simplest model for bus movement is constituted by assuming constant speed v_s
 14 for the travel between stops s and $s + 1$ leading to travel time $\widehat{TT}_{i,s} = (X(s + 1) - X(s) - 2G)/v_s$
 15 for trip i on route segment s and non-negative stopping times $\widehat{ST}_{i,s}$ inside the stop. For a shape with
 16 S stops (not counting the start of the trip) this leads to $2S$ parameters. For this model $\widehat{TT}_{i,s}, \widehat{ST}_{i,s}$
 17 and the time $t_{i,1}$ of the start of the trip fully determine the trajectory of the bus according to

$$\hat{t}(x) = t_{i,1} + \sum_{s: X(s) < x} (\widehat{TT}_{i,s} + \widehat{ST}_{i,s}) + \frac{x - X(s) - G}{X(s + 1) - X(s) - 2G} \widehat{TT}_{i,s+1} \quad (1)$$

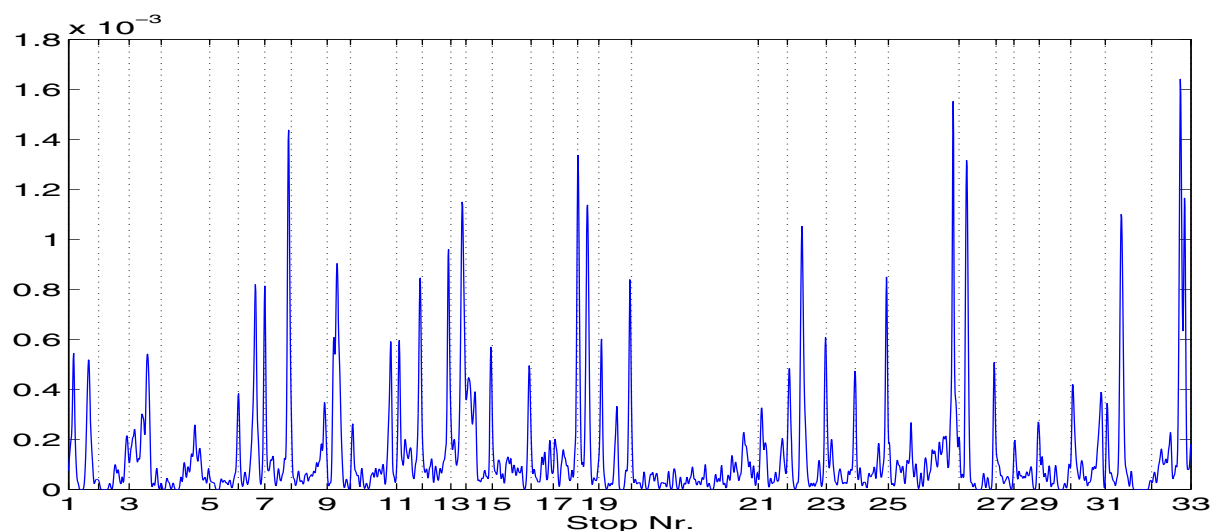


FIGURE 2 Kernel density estimator for observed location of buses of route 1 in Boston in the inbound direction. Dashed lines indicate places of stops.

1 for each $x \notin [X(s) - G, X(s) + G]$ not in a stop. Inside the stops linear progression between entering
 2 the interval and exiting the interval can be assumed without loss of generality.

3 This model needs to be calibrated with real world data in order to be useful. In this respect
 4 the following observation will be used: For an observer that searches for the location of a bus at
 5 a random time instant, the chance to find the bus in an interval of 10m, say, is proportional to the
 6 share of time the bus spends in this interval during the observation period. The same holds true for
 7 more frequent sampling of bus location. Fig. 2 provides a snapshot of the location of observations
 8 of buses on route 1 in the inbound direction (i.e. in direction of Harvard).

9 It can be seen that at some stops buses are more frequently found. Other spikes occur at
 10 traffic lights. This can be related to average dwell time percentages \bar{ST}_s inside the stop intervals as
 11 well as on the segments between the stops.

12 In order to calibrate this model the observations are split into two groups: Observations
 13 in the stops $[X(s) - G, X(s) + G]$ are termed in-stop observations and denoted as $z_{i,k}, k = 1, \dots, K$
 14 with corresponding time $t_{i,k}$ and stop $s_{i,k}$. The remaining ones are termed on-road observations and
 15 denoted as $y_{i,l}, l = 1, \dots, L$ with corresponding time $t_{i,l}$ and segment $s_{i,l}$. In-stop observations im-
 16 pose restrictions as $\hat{t}(X(s_{i,k}) - G) \leq t_{i,k}$ and $\hat{t}(X(s_{i,k}) + G) \geq t_{i,k}$, i.e. the trip must arrive at the stop
 17 prior to being observed in the stop and depart after being observed there. The on-road observations
 18 should be replicated as good as possible using the model. From the assumption of constant speed
 19 between stops it is clear that there will be no perfect match in particular in situations where the bus
 20 needs to wait at a traffic light.

21 At the same time we want the model to match the dwell time profile as closely as possible.
 22 Hence the re-sampling is achieved by finding the parameters minimizing the squared distance to
 23 the scaled (with the actual total travel time TTT_i for the whole trip) dwell time profile and the
 24 weighted on-road observations subject to the restrictions on arriving and departure times implicit
 25 in the on-stop observations:

1

$$\begin{aligned}
\min L(t_{i,1}, \widehat{TT}_{i,s}, \widehat{ST}_{i,s}, s = 1, \dots, S) &:= \sum_{l=1}^L (t_{i,l} - \hat{t}(y_{i,l}))^2 + w \sum_{s=1}^S (\widehat{ST}_{i,s} - TTT_i * \bar{ST}_s)^2, \\
s.t. \quad \hat{t}(X(s_{i,k}) - G) &\leq t_{i,k}, \\
\hat{t}(X(s_{i,k}) + G) &\geq t_{i,k}, k = 1, \dots, K, \\
\widehat{TT}_{i,s} &\geq (X(s+1) - X(s) - 2G)/V, s = 1, \dots, S, \\
\widehat{ST}_{i,s} &\geq 2G/V, s = 1, \dots, S.
\end{aligned} \tag{2}$$

2 Here $w > 0$ is a weighting factor. Large w results in closer fit to the average dwell times,
3 small w puts emphasis on being close to measured observations. V imposes a maximal travel speed.
4 This leads to a linear least squares problem with linear restrictions which can be efficiently solved
5 using general purpose optimizers.

6 The re-sampling procedure uses the assumption that the expected dwell times are identical
7 for all buses, i.e. that there are no systematic deviations from the expectations. This is not realistic
8 for a full day, while it appears tenable for time intervals across different days. Consequently we
9 calculate the re-sampling separately for a segmentation of the day into ten time intervals.

10 Below the re-sampling procedure is validated using synthetic as well as real world data.

11 2.2.1 Validation Using Synthetic Data

12 In order to validate the re-sampling procedures a synthetic data set of buses running on route 1 has
13 been generated using a microscopic simulator implementing the optimal velocity model (OVM)
14 as presented in [12] with a discrete time update of one second and a total duration of 10 hours.
15 Only one direction with no overtaking is simulated. The shape contains 33 bus stops. If a bus
16 reaches a stop, a random integer is drawn simulating uncertain boarding and alighting processes.
17 The stop duration is distributed discretely uniform $\{0, 1, 2\}$ seconds except for stops 6, 21 and 31
18 where the range is 30 to 149 seconds and stops 7 to 20, where the range is 5 to 19. On the route
19 twenty intersections with traffic signals are simulated. The signal timing is coordinated using the
20 maximum allowed speed with red and green time split evenly at 30 seconds each. During the red
21 light periods of signal 2, 7, 12, 17 and 18 cars enter the road segment with intensity $t/36000 * 0.75$
22 according to a Poisson arrival process. Other than that cars enter the road at the start of the shape
23 at an arrival rate of 0.2. Every three minutes a bus is drawn. The stopping of a bus in a stop is
24 not modelled in detail, but rather buses stop immediately when reaching the stop and leave after
25 boarding and alighting is completed. In between cars pass the bus. The added complexity of
26 deceleration into the stop is included in the random boarding and alighting, the reintegration into
27 traffic follows the rule that cars need to stop for reentering buses.

28 195 bus trajectories are generated at a sampling frequency of one second. Subsequently the
29 trajectories are sub-sampled to a sampling frequency of sixty seconds using random starting time
30 stamp. The two re-sampling strategies (simple linear as well as the procedure proposed above) are
31 applied and stopping times as well as travel times between bus stops are calculated with the two
32 approaches. For the distribution based re-sampling the 10 hours are partitioned into three intervals.
33 A sample of the output of the resampling procedure can be found in Figure 3 below. It can be seen
34 that the resampling follows the true observations more closely than linear interpolation.

35 The results show that the more complicated re-sampling pays off resulting in a smaller
36 mean absolute deviation for stop duration of 8.8 seconds compared to 11.2 seconds for the simple

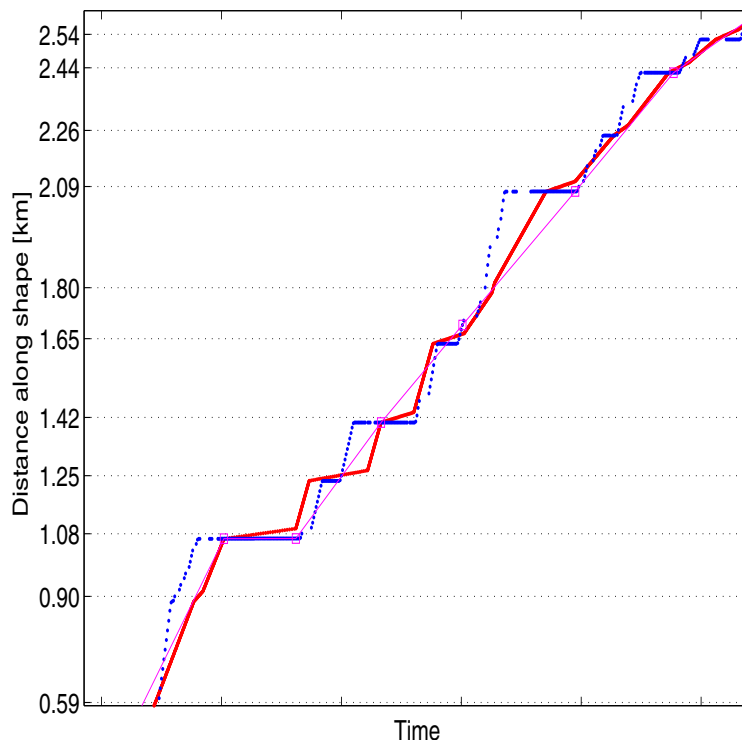


FIGURE 3 MBTA route 1: Sample output of the resampling scheme. Blue dots: high frequent observations. Magenta boxes: Observations with sixty second temporal resolution. Thin magenta line: linear resampling. Thick red line: Proposed resampling.

1 linear interpolation based re-sampling. Also the travel times between the stops are replicated with
 2 a higher accuracy (mean absolute deviation of 10.3 compared to 12.0 second). Additionally note
 3 that the absolute performance is high in comparison to the sampling interval 60 seconds. This is
 4 mainly due to a better capturing of the long stops. For the three long stops 6, 21 and 31 the mean
 5 absolute deviation of our re-sampling equals 21.4 seconds compared to 46.3 seconds for the simple
 6 method.

7 2.2.2 Validation Using High-Frequency GPS Data

8 In order to validate our methodology, we collected high-frequency GPS records with a sampling
 9 frequency of one second on bus line 1 on two days, Thursday February 23rd 2012 and Saturday
 10 February 25th. A total of 15 trips provide data which is map matched and converted to sequences
 11 of (time stamp, distance along shape) pairs. The one second interval GPS data provides ground
 12 truth against which the two sampling strategies are validated. To this end the trips are separated
 13 into different regimes according to weekend or weekday as well as five intervals during the day.

14 The two re-sampling schemes have been applied to sub-sampled (using each sixtieth obser-
 15 vation) copies of each of the 15 trips. In order to remove random effects due to the starting point
 16 all 60 sub-sampled versions are used.

17 The results are less pronounced than for the synthetic data but still an advantage of the
 18 more complex re-sampling scheme compared to the simple method can be observed. The mean
 19 absolute deviation in stopping time over all stops in direction 1 totals 4.83 seconds for the present-

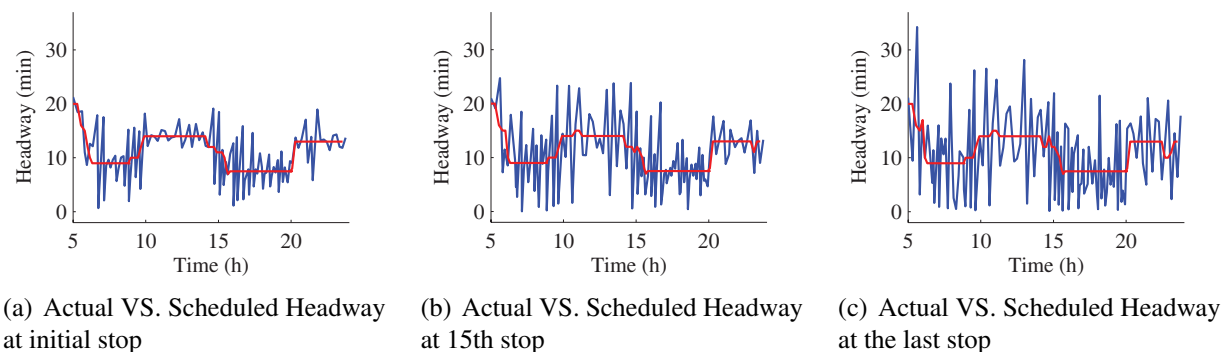


FIGURE 4 Actual vs. scheduled headway at the initial, the middle and the last stops.

1 ed re-sampling method and 7.7 seconds for the simple interpolation. In direction 0 the numbers
 2 of 6.5 for our method compared to 7.7 for the simple method results in a slight advantage of the
 3 proposed method.

4 Note in this respect that the errors are comparable but smaller than in the synthetic data set.
 5 Thus, in the following the presented re-sampling method will be used.

6 3 ANALYSIS OF SERVICE QUALITY

7 The resampled data represents a great opportunity to make statistics of the bus service performance.
 8 The usual service quality measurements relate strongly to variations of headway, travel time and
 9 variability of travel time. Transit operators are interested to optimize indicators based on these
 10 components which include elements not under the influence of the transit operators such as traffic
 11 conditions and demand fluctuations. In this section we demonstrate that the resampled data set
 12 can be used in order to extract useful information about these three components of service quality
 13 measurement.

14 Headway

15 Headway is defined as the time interval from the tip of one vehicle to the tip of the next one behind
 16 it arriving at a certain place (usually a stop). The expectation μ and the variance σ^2 of headway
 17 influence expected waiting times at stops according to the following formula (see [13]):

$$W = \mu \times \frac{(1 + \frac{\sigma^2}{\mu^2})}{2} \quad (3)$$

18 For MBTA route 1, Fig. 4(a) to Fig. 4(c) show how the actual headways compare to the
 19 scheduled ones at the initial stop, the 15th stop, and the last stop on one of the workdays. We define
 20 the headway deviation as the difference between the actual headway and the scheduled headway.
 21 Even at the initial stop the deviations are significant. The deviations at the initial stop are caused
 22 by operation issues: either because there are buses available at the terminal but the operators fail
 23 to dispatch them in time, or because bus slack time at the terminal is not enough so that buses are
 24 not ready at their scheduled departure time.

25 To explore how headway changes from the first to the last stop consider the evening peak
 26 headway. We calculate the headway distribution at each stop and fit various distributions such as
 27 exponential, Erlang, gamma and normal distribution [14, 15]. We observed that the best statistical

1 fit was obtained by the three parameter gamma distribution which is recommended by the traffic
 2 engineering handbook [16]: The corresponding probability density function equals

$$f(x) = \frac{(x - \gamma)^{\alpha-1}}{\beta^\alpha \Gamma(\alpha)} \exp(-(x - \gamma)/\beta), x \geq \gamma, f(x) = 0, x < \gamma. \quad (4)$$

3 Here $\alpha > 0$ is the continuous shape parameter. When α is 1 the distribution becomes an
 4 exponential distribution and when α is 4 or 5 the shape is close to a normal distribution. $\beta > 0$ is
 5 the continuous scale parameter. The larger the scale parameter, the more spread out the distribution
 6 is. γ is the continuous location parameter which determines the center of the distribution. Γ is the
 7 Gamma function.

The comparison of headway histograms and fitted distributions are shown in Fig. 5. The

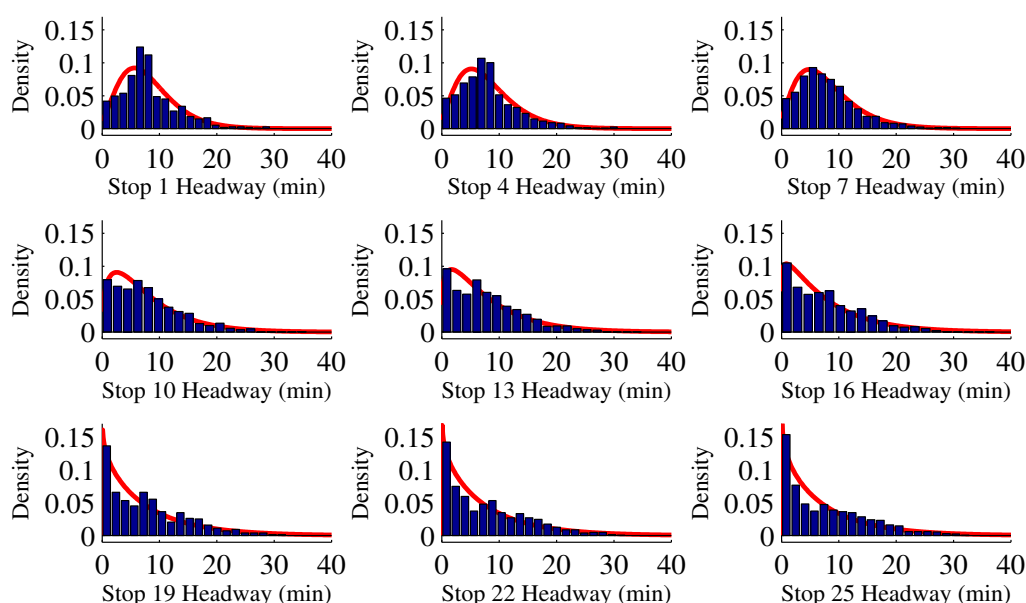


FIGURE 5 Headway fitting results at different stops using the three parameter gamma distribution.

8
 9 three parameter gamma distribution fits quite well from the initial stop to the last stop. Fig. 6
 10 shows how the three parameters change from the first to the last stop. At the initial stop, the shape
 11 parameter is close to 4 which shows that it is relatively close to a normal distribution. The shape
 12 parameter decreases quickly along the route. After stop 9 it stabilizes at around 1 which indicates
 13 that it is close to an exponential distribution. The location parameter also stabilizes at around 0
 14 after stop 9. This means that after stop 9 a large proportion of headways are close to 0, which
 15 indicates that bus bunching is severe. After the shape and the location parameter stabilize, the
 16 scale parameter keeps increasing which shows that the variance of headway keeps increasing.

17 To further understand the headway variations, we calculated the headway coefficient of
 18 variation C_{vh} , a measurement proposed in TCQSM [17], at different stops:

$$C_{vh} = \frac{\text{Standard deviation of headway deviations}}{\text{Mean scheduled headway}} \quad (5)$$

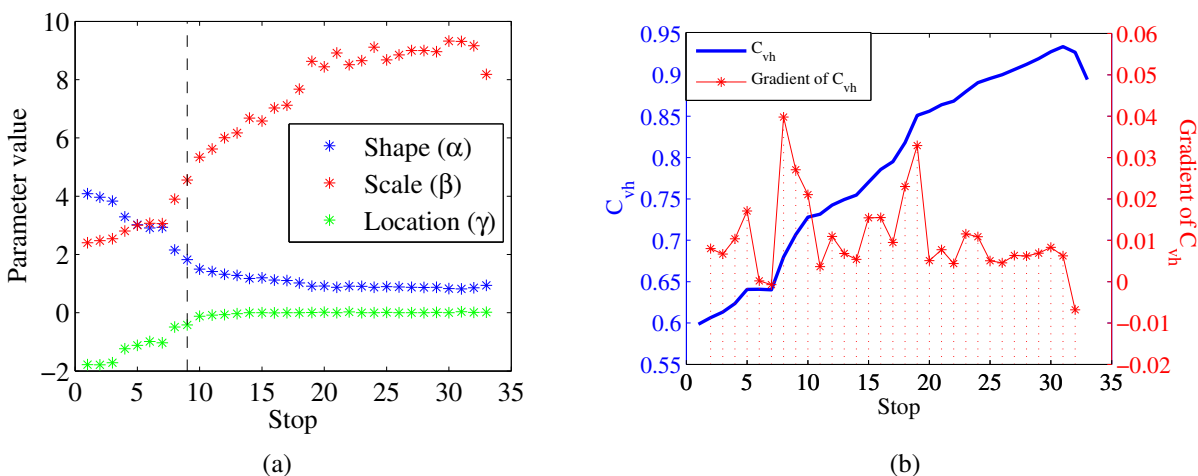


FIGURE 6 (a) Evolution of the parameters of the gamma distribution across the bus route during the evening peak. (b) Headway coefficient of variation (left axis) and its gradient (right axis) showing bottlenecks with high headway variation increase at stop 9 and 19.

1 Fig. 6(b) shows how the headway coefficient of variation at each stop changes along the
 2 route. The general trend is that the headway coefficient of variation keeps increasing, but the rate
 3 of increase varies from stop to stop. Between some stops it increases more quickly, which shows
 4 that in these segments travel times (between arriving at consecutive stops) are more unstable. In
 5 order to observe the change rate, the gradient of headway coefficient of variation at each stop is
 6 shown in Fig. 6 (b). At stops 8 and 19 it increases the most. Inspection from the map shows
 7 that between stop 8 and 9 the bus turns from a secondary road (Albany St.) to the main artery
 8 connecting Boston and Cambridge (Massachusetts Avenue). The traffic signal waiting time at this
 9 intersection could vary a lot which causes higher headway variance. Bus priority at this intersection
 10 hence could greatly increase headway regularity. Between stop 18 and 19 there are three closely
 11 spaced intersections. The Metro Green line also transfers with route 1 at stop 18. Hence both
 12 the waiting times at intersections and varying passenger flows make the headway unstable here.
 13 Two possible ways to improve the service quality are better bus priorities at these traffic lights and
 14 holding strategies in order to better synchronize buses and the metro line.

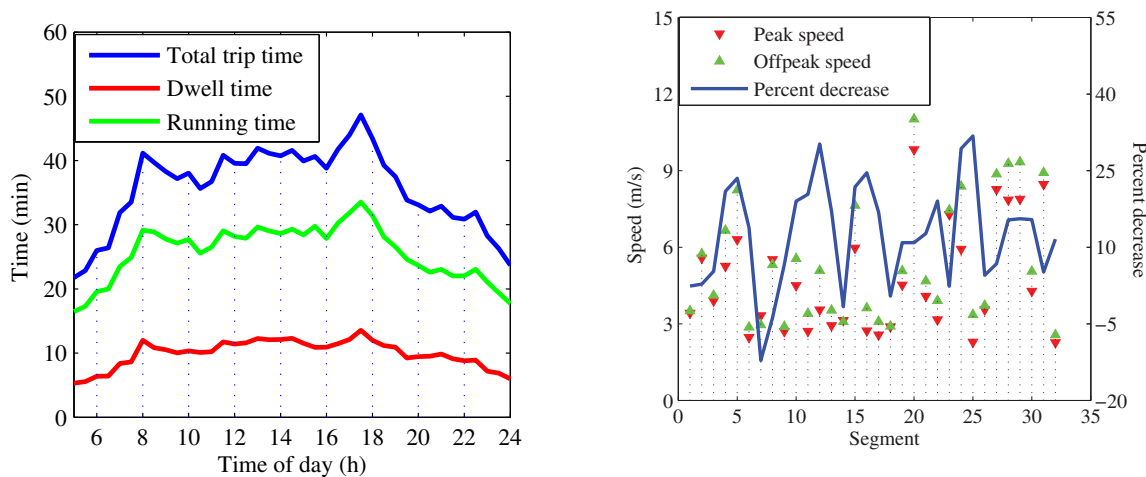
15 **In-vehicle travel time**

16 Another component of the total travel time is in-vehicle travel time which is composed of two part-
 17 s: travel time between stops and stop dwelling time. In-vehicle travel time is largely determined by
 18 traffic conditions and the road network structure. Fig. 7(a) shows how the average total trip time,
 19 running time and stop dwelling time change during different times of day. The total trip time has
 20 clear morning and evening peaks at 8am and 5:30pm respectively. Running time and stop dwell
 21 time show identical peaks, which means that the increase in the total peak trip time is caused by
 22 both increasing passenger volumes and slower travel speed. Running time has a larger influence
 23 on the increase of the total peak trip time.

24 Fig. 7(b) compares the average travel speed (stop dwell time not included) and the percent-
 25 age decrease from off-peak to peak hours at each segment. Segment i is the road between stop i
 26 and $i + 1$. At segment 20 the average speed is always the highest because this segment is at Harvard

1 bridge and on the bridge there are no traffic lights or stops. The peak hour speed is generally lower
 2 than the off-peak hour speed. The highest percentage decreases are at segment 12 and 25 which are
 3 respectively at the intersection of Massachusetts Avenue and Tremont St. and at Central Square,
 4 both crowded commercial areas in Boston and Cambridge respectively.

It is interesting to notice that stops with the most percentage decrease in peak hour speed



(a) Trip time composition at different times of day. Values represent the sum over the entire route.

(b) Average Speed during peak/ off-peak periods. The solid line shows the speed percentage decrease in peak hours.

FIGURE 7 Trip time at different times of day and peak/ off-peak travel speed comparison.

5 do not correspond to stops where the statistics of headway varies the most. This is because the
 6 headway coefficient of variation is a measurement of stability while the in-vehicle travel time is a
 7 measurement of the average speed performance.
 8

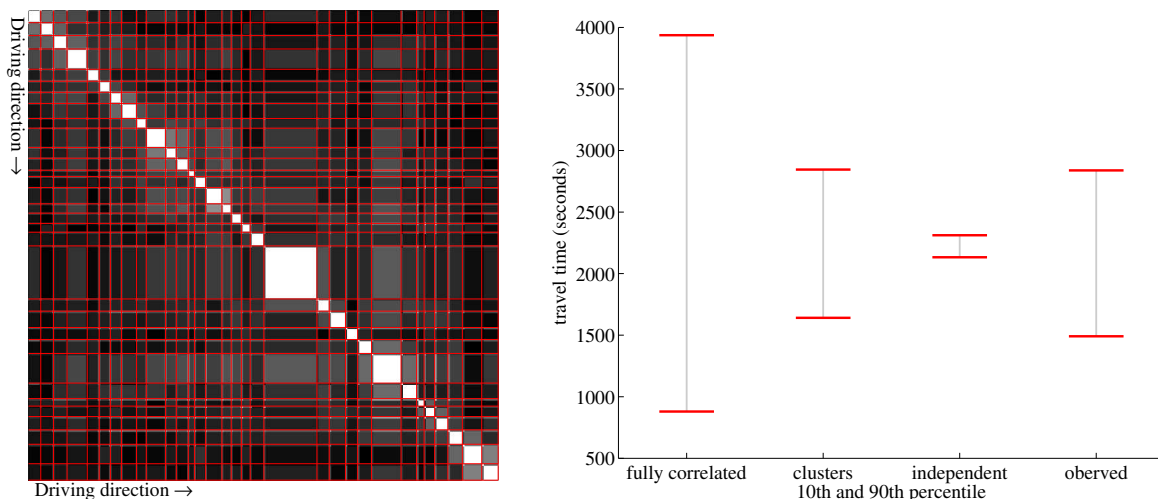
9 **Variability of trip travel time**

10 Another component of bus performance is constituted by travel time variability. High variability
 11 implies low predictability and hence uncertain travel times. Thus alongside the expected travel
 12 time, travel time reliability is one of the most important factors when selecting a route to a desired
 13 destination. The expected travel time can be calculated easily by summing up the mean segment
 14 travel times along the route in the transportation network. On the other hand, in order to estimate
 15 variability, it is necessary to account for correlations between the individual segments compos-
 16 ing the trip. Figure 8(a) shows the correlation matrix of the segment travel times along the bus
 17 route. The probability distribution of the trip travel time can be approximated by building clusters
 18 of highly correlated segments and assuming full correlation within each cluster and independence
 19 between segments in different clusters. The quantile function, i.e. the quasi-inverse of the cumula-
 20 tive distribution function (CDF), of the sum of fully correlated segment travel times $\widehat{TT}_s, s \in C$ in
 21 cluster C is computed as the sum of the quantile functions of the individual constituents, i.e.

$$Q_C(p) = \sum_{s \in C} Q_{\widehat{TT}_s}(p) \tag{6}$$

22 where $Q_C(p)$ denotes the p -th ($0 \leq p \leq 100$, percent) quantile of the travel time for cluster C . The
 23 distribution of the sum of independent cluster travel times is approximated by Monte Carlo simu-

1 lation, where cluster travel times are drawn repeatedly and randomly according to the previously
 2 calculated probability distributions of the respective clusters. Figure 8(b) compares the resulting
 3 estimations with empirical travel time distributions for trips from the first to the last stop of MBTA
 4 route 1. For comparison, also depicted are the results under the assumption that all segments are
 5 independent and assuming that every segment is fully correlated with every other. These result-
 6 s show that not accounting for dependencies leads to underestimation of travel time variability,
 7 whereas the proposed approximation yields good agreement with the observed distribution. Thus
 8 the low frequency localization data can be used in order to infer route travel time reliability for
 9 arbitrary routes along the line providing another way to investigate bus performance.



(a) Correlation matrix of segment travel times on MBTA Route 1. White indicates high correlation and black indicates low correlation. Red lines mark the positions of stops.

(b) From the left to the right: the spread between the 10th and 90th percentile of the estimated travel time distribution assuming (a) full correlation between all segments, (b) full correlation within and independence between segment clusters, (c) independence between all segments and (d) the observed travel time distribution.

FIGURE 8 Correlation between segment travel times and comparison of estimated travel time under various assumptions to observed travel time.

10 **4. APPLICATION: CALIBRATION OF A BUS MOVEMENT MODEL**

11 Beside performing service quality analysis and bottleneck diagnosis, transit agencies may be in-
 12 terested to evaluate the effect of different measures to improve service quality. In this section we
 13 show that the headway and the travel time statistics calculated in the previous section can be used
 14 to calibrate bus movement simulation models.

15 The bus' movement is affected by traffic conditions, traffic signals and the number of pas-
 16 sengers boarding and alighting. The number of passengers is both related to passenger arrival rates
 17 and the arrival time of the previous bus. In Daganzo [18] a very convenient bus movement model
 18 is built incorporating the effect of the previous bus and the random noise caused by road condi-
 19 tions and traffic signals. Using the measured statistics of service performance we can calibrate this
 20 model.

1 **4.1. The model**

2 The bus movement model of [18] can be expressed as:

3

$$U_{n,s} = C_s + \beta_s(h_{n,s} - H) + v_{n,s+1} \tag{7}$$

4

5 Here $U_{n,s}$ is the n th run's segment travel time from stop s to $s + 1$. The dwell time at stop
 6 s is included while the dwell time at stop $s + 1$ is not. C_s is the scheduled travel time from s to
 7 $s + 1$. H is the scheduled headway while $h_{n,s}$ is the actual headway for the n th run at stop s . β_s is a
 8 dimensionless parameter expressing the effect of the deviation from the scheduled headway on the
 9 dwell time. If a headway is longer than the scheduled value and the passenger arrival rate remains
 10 constant, there will be more passengers arriving than expected which causes longer than expected
 11 stop dwell time. The inclusion of β_s makes two buses "attract" each other when their headway is
 12 shorter than H and "repel" each other when the headway is longer than H . In Daganzo [18], it is
 13 mentioned that β_s typically ranges from 10^{-2} to 1. The noise term $v_{n,s+1}$ incorporates effects such
 14 as road conditions and traffic signals. It is assumed to have zero mean, variance σ_{s+1}^2 and to be
 15 independent of h_{ns} .

16 If we use $a_{n,s}$ to represent the arrival time of the n th run at stop s the above equation could
 17 be transformed as:

18

$$a_{n,s+1} - a_{n,s} = C_s + \beta_s(a_{n,s} - a_{n-1,s} - H) + v_{n,s+1} \tag{8}$$

19 **4.2. Model calibration**

20 As $a_{n,s+1}$, $a_{n,s}$, and $a_{n-1,s}$ can be acquired directly from our interpolated data, estimates of β_s can
 be obtained using regression.

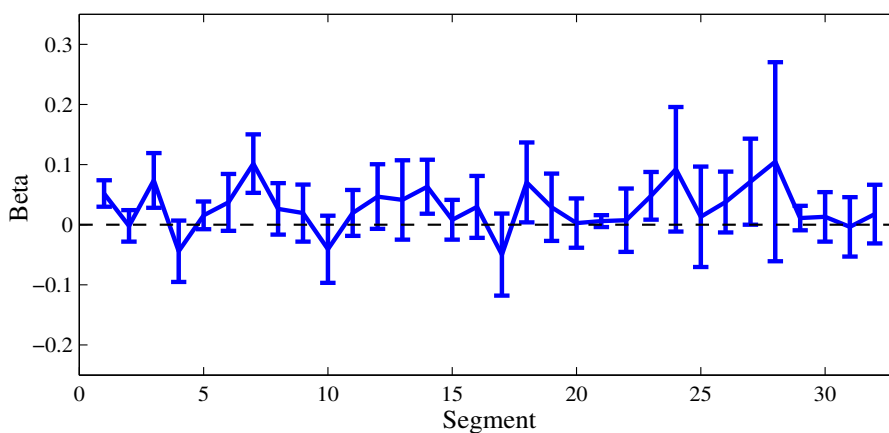


FIGURE 9 Regression result of β_s (see equation (7)) at each segment.

21

22 The regression results with error bars, provided in Fig. 9, show the expected positive signs
 23 for 27 out of 32 segments. None of the negative coefficients are significant. These values all agree
 24 with the typical β_s values indicated in Daganzo [18]. Note that the low number of significant
 25 coefficients may be an indication of insufficient sample size and hence small power of the tests.

26

Notice that with the interpolated AVL data we have all the components needed for the

1 movement simulation model. C_s and H can be acquired from the schedule. Headway distributions
 2 using the Gamma family of densities have been fitted above, v_{s+1} is approximated using a log-
 3 normal distribution. Fig. 10 provides a comparison between simulated and true segment travel
 4 time distributions. Kolmogorov-Smirnoff test statistics have been calculated in order to compare
 5 the accuracy of the simulations using a log-normal distribution (red lines) and a normal (green
 6 broken lines) distribution for the random noise term. It can be observed that for all segments
 7 except the first one the fit of the distribution for the lognormal distributed noise is acceptable as the
 8 KS test has for confidence level 95% and the sample size used a critical value of 0.07.

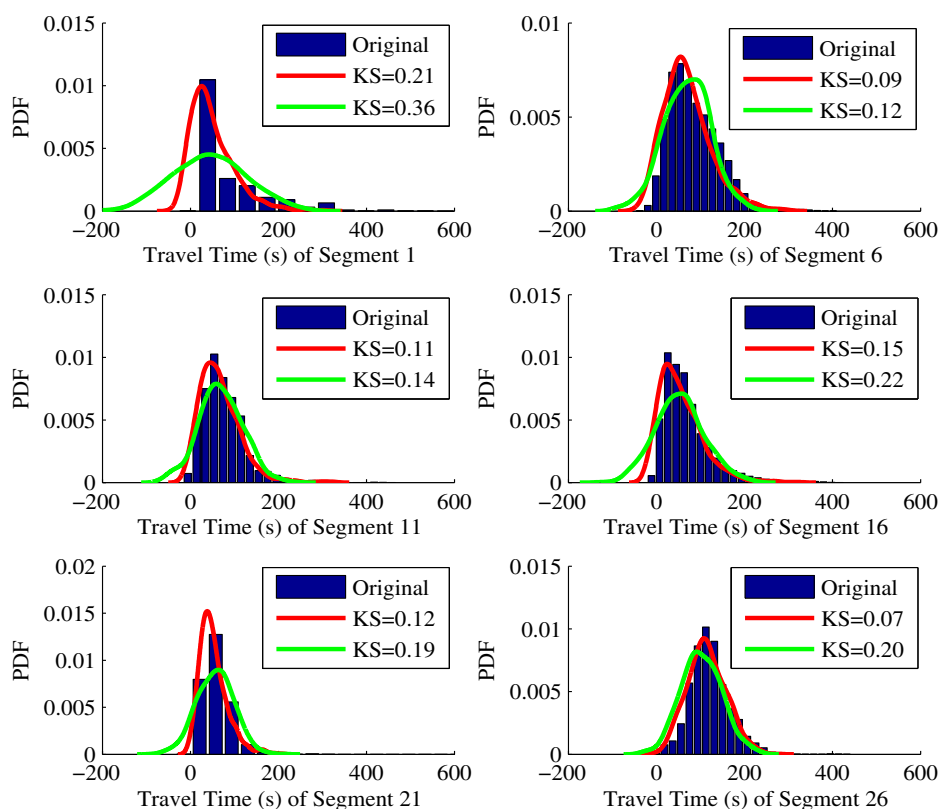


FIGURE 10 Comparison of bus travel time (U_s) at different segments of the route. We present the original data and two simulated bus models. One (green dashed line) assuming normally distributed random noise term and the other one (red solid line) calibrated with the statistical distributions observed in this study. Kolmogorov-Smirnov test values are shown on the legends.

9 **5. CONCLUSIONS AND OUTLOOK**

10 In this paper we propose a low-frequency AVL data analysis procedure which allows service per-
 11 formance evaluation and the calibration of a bus movement model. It is demonstrated how low-
 12 frequency location-at-time AVL records as provided e.g. by Nextbus can be used in order to obtain
 13 useful information on bus service performance. In particular the main contributions of this study

1 to the state-of-the-art research can be concluded as:

- 2 1. A more robust and accurate data preprocessing methodology is provided which is demon-
3 strated to be superior to the widely applied linear interpolation method. More accurate
4 stop arrival and departure time estimates are obtained by using a kernel density estimator
5 of bus dwell time.
- 6 2. Using this preprocessing method, headway distribution evolution along one bus route
7 is studied in detail. It is demonstrated that the method can be used in order to detect
8 bottlenecks caused by both road layout and traffic conditions separately so that they can
9 be treated differently to improve service quality.
- 10 3. Route travel time variability can be inferred from clustering of segments based on seg-
11 ment travel time correlations. This delivers hints on bus performance problems via
12 increases in variability thus providing a more complete view on the performance of the
13 bus line.
- 14 4. These results can be used to calibrate bus simulation models which in turn can be further
15 applied to evaluate various bus control strategies.

16 Therefore the paper demonstrates the potential of widely available (and hence low cost) low-
17 frequency AVL data to improve bus service and to provide valuable information for the passen-
18 gers in terms of travel time predictions including travel time reliability. In particular we show that
19 such data provides an alternative means for monitoring and controlling bus performance for transit
20 authorities not willing to invest in more expensive solutions.

21 **ACKNOWLEDGEMENTS**

22 The authors thank Nextbus for providing access to the data as well as the MBTA for discussions
23 on the results. Also seminar participants of the Transit Research group at MIT provided valuable
24 inputs into the paper which is gratefully acknowledged.

25 **REFERENCES**

- 26 [1] Furth, P., B. Hemily, T. Muller, and J. Strathman, TCRP report 113: Using archived AVL-
27 APC data to improve transit performance and management. *Transportation Research Board*
28 *of the National Academies, Washington, DC, 2006.*
- 29 [2] Kimpel, T., J. Strathman, and S. Callas, Improving Scheduling Through Performance Moni-
30 toring. *Computer-aided Systems in Public Transport, 2008, pp. 253–280.*
- 31 [3] Byon, Y., C. Cortés, C. Martinez, F. Javier, M. Munizaga, and M. Zuniga, Transit Perform-
32 ance Monitoring and Analysis with Massive GPS Bus Probes of Transantiago in Santia-
33 go, Chile: Emphasis on Development of Indices for Bunching and Schedule Adherence. In
34 *Transportation Research Board 90th Annual Meeting, 2011, 11-2233.*
- 35 [4] Cortés, C., J. Gibson, A. Gschwender, M. Munizaga, and M. Zúñiga, Commercial bus speed
36 diagnosis based on GPS-monitored data. *Transportation Research Part C: Emerging Tech-*
37 *nologies, 2011.*

- 1 [5] Lee, D., L. Sun, and A. Erath, Study of Bus Service Reliability in Singapore Using Fare Card
2 Data. In *The 12th Asia Pacific ITS Forum*, 2012.
- 3 [6] Cham, L., Understanding bus service reliability: a practical framework using AVL/APC data.
4 In *MS Thesis, Prof. Nigel Wilson, Massachusetts Institute of Technology*, 2006.
- 5 [7] Abkowitz, M. and J. Tozzi, Research contributions to managing transit service reliability.
6 *Journal of advanced transportation*, Vol. 21, No. 1, 1987, pp. 47–65.
- 7 [8] Abkowitz, M., *Transit service reliability*, 1978.
- 8 [9] Pangilinan, C., N. Wilson, and A. Moore, Bus supervision deployment strategies and use
9 of real-time automatic vehicle location for improved bus service reliability. *Transportation*
10 *Research Record: Journal of the Transportation Research Board*, Vol. 2063, No. -1, 2008,
11 pp. 28–33.
- 12 [10] Hickman, M., An analytic stochastic model for the transit vehicle holding problem. *Trans-*
13 *portation Science*, Vol. 35, No. 3, 2001, pp. 215–237.
- 14 [11] Quddus, M., W. Ochieng, and R. Noland, Current map-matching algorithms for transport
15 applications: State-of-the art and future research directions. *Transportation Research Part C:*
16 *Emerging Technologies*, Vol. 15, No. 5, 2007, pp. 312–328.
- 17 [12] Treiber, A. and M. Kesting, *Verkehrsdynamik und -simulation*. Springer, 2010.
- 18 [13] Holroyd, E. and D. Scraggs, *Waiting times for buses in central London*. Printerhall, 1966.
- 19 [14] Gentile, G., S. Nguyen, and S. Pallottino, Route choice on transit networks with on-line
20 information at stops. *Transportation Science, Technical Report TR-03-14, Universitadi Pisa,*
21 *Dipartimento di Informatica, Pisa, Italy*, 2003.
- 22 [15] Bellei, G. and K. Gkoumas, Transit vehicles headway distribution and service irregularity.
23 *Public Transport*, Vol. 2, No. 4, 2010, pp. 269–289.
- 24 [16] Pline, J., *Traffic engineering handbook*. Prentice Hall, 1992.
- 25 [17] Kittelson Associates, Inc., KFH Group, Inc., Parsons Brinckerhoff Quade, Douglass, Inc.,
26 and K. Hunter-Zaworski, *TCRP Report 100: Transit Capacity and Quality of Service Manual*.
27 Transportation Research Board, 2003.
- 28 [18] Daganzo, C., A headway-based approach to eliminate bus bunching: Systematic analysis and
29 comparisons. *Transportation Research Part B*, Vol. 43, 2009, pp. 913–921.